# Theoretical characterization of titanyl phthalocyanine as a p -type organic semiconductor: Short intermolecular π π interactions yield large electronic couplings and hole transport bandwidths

Joseph E. Norton and Jean-Luc Brédas

Citation: The Journal of Chemical Physics **128**, 034701 (2008); doi: 10.1063/1.2806803
View online: http://dx.doi.org/10.1063/1.2806803
View Table of Contents: http://scitation.aip.org/content/aip/journal/jcp/128/3?ver=pdfcov
Published by the AIP Publishing

# Theoretical characterization of titanyl phthalocyanine as a *p*-type organic semiconductor: Short intermolecular $\pi$-$\pi$ interactions yield large electronic couplings and hole transport bandwidths

Joseph E. Norton and Jean-Luc Brédas[a)]
*School of Chemistry and Biochemistry, Georgia Institute of Technology, Atlanta, Georgia 30332-0400, USA and Center for Organic Photonics and Electronics, Georgia Institute of Technology, Atlanta, Georgia 30332-0400, USA*

(Received 25 July 2007; accepted 16 October 2007; published online 15 January 2008)

The charge-transport properties of the triclinic phase II crystal of titanyl phthalocyanine ($\alpha$-TiOPc) are explored within both a hopping and bandlike regime. Electronic coupling elements in convex- and concave-type dimers are calculated using density functional theory, and the relationship between molecular structure and crystal packing structure in model dimer configurations is considered. Hole transport bandwidths derived from crystal structure dimers are compared to those obtained from electronic band structure calculations; very good agreement between the two approaches is found. The calculations predict large hole bandwidths, on the order of 0.4 eV, and correspondingly very low hole reorganization energies. © *2008 American Institute of Physics*. [DOI: 10.1063/1.2806803]

## I. INTRODUCTION

Phthalocyanines are a versatile class of $\pi$-conjugated organic semiconductors applicable as materials in many electronic devices such as organic xerographic photoreceptors,[1] nonlinear optical components,[2] field-effect transistors,[3] organic light-emitting diodes,[4] and solar cells.[5,6] Titanyl phthalocyanine (TiOPc), in particular, has become of interest because of its semiconducting as well photoconductivity[1] and third-order nonlinear optical properties.[7] As in other phthalocyanines, the absorption spectrum,[8,9] photoconductivity,[1] photodynamic behavior,[10] and charge-transport properties of TiOPc vary substantially depending on the crystal phase it adopts in the solid state. TiOPc is known to form various polymorphs that are responsible for differences in stacking modes and molecular alignment in ordered solid films.[9] Of the various polymorphs of TiOPc, the so-called Y-form (Y-TiOPc) is one of the most efficient photoconducting materials,[1,11] while the triclinic phase II ($\alpha$-TiOPc) is an excellent *p*-type semiconductor with a broad spectral absorption range suitable for use in solar cells.[6] As indicated by variations in the solid-state properties of different TiOPc polymorphs, molecular stacking arrangements have a profound influence on the electronic properties. This underscores the overall importance of establishing well-understood relationships between molecular structure, crystal packing structure, and charge transport in organic materials.

The performance of novel electronic devices made of organic semiconductors depends largely on their ability to efficiently transport charges. Organic light-emitting diodes, field-effect transistors, and solar cells rely on charge-transport characteristics that can be described at the molecular level by several factors such as electronic coupling, vibronic interactions, and relative energies of the charge-transfer reactants and products. Organic materials based on small-molecule crystals or polymers require strong interactions between neighboring molecules or moieties, a factor that is determined by the crystal structure of the system and known to substantially affect carrier mobility. Therefore, it is important to understand how differences in crystal packing and, in many cases, disorder influence fundamental charge-transfer parameters such as electronic coupling.

Whether transport occurs through a bandlike or hopping mechanism, the charge carrier mobility is determined by electronic coupling. Charge transport in most organic materials occurs through a charge hopping mechanism, where an electron hop corresponds to an electron-transfer reaction. In the semiclassical approximation, or high-temperature limit, Marcus theory has been used extensively to study the effects of molecular and crystal structures on charge-transport parameters.[12] The Marcus electron-transfer rate is expressed as[13]

$$k_{ij} = \frac{2\pi}{\hbar}|V_{ij}|^2 \frac{1}{\sqrt{4\pi k_B T}} \exp\left(-\frac{(\lambda_{ij} + \Delta G^0)^2}{4\lambda_{ij} k_B T}\right), \quad (1)$$

where $V_{ij} = \langle \psi_i | H | \psi_j \rangle$ is the electronic coupling matrix element (or transfer integral) of the system Hamiltonian between the initial and final states $|\psi_i\rangle$ and $|\psi_j\rangle$, $\lambda_{ij}$ is the reorganization energy, and $\Delta G^0$ is the change in Gibbs free energy for the electron-transfer reaction. This type of model is usually appropriate for organic materials since contributions from electronic coupling and vibrational relaxations are taken into account.

If electron-phonon coupling is weak, a bandlike regime can manifest in perfectly ordered systems at low temperature. The band regime can be considered within a simple tight-binding model in which the total valence bandwidth ($W$) results from interaction of the highest occupied molecu-

[a)]Electronic mail: jean-luc.bredas@chemistry.gatech.edu.

 

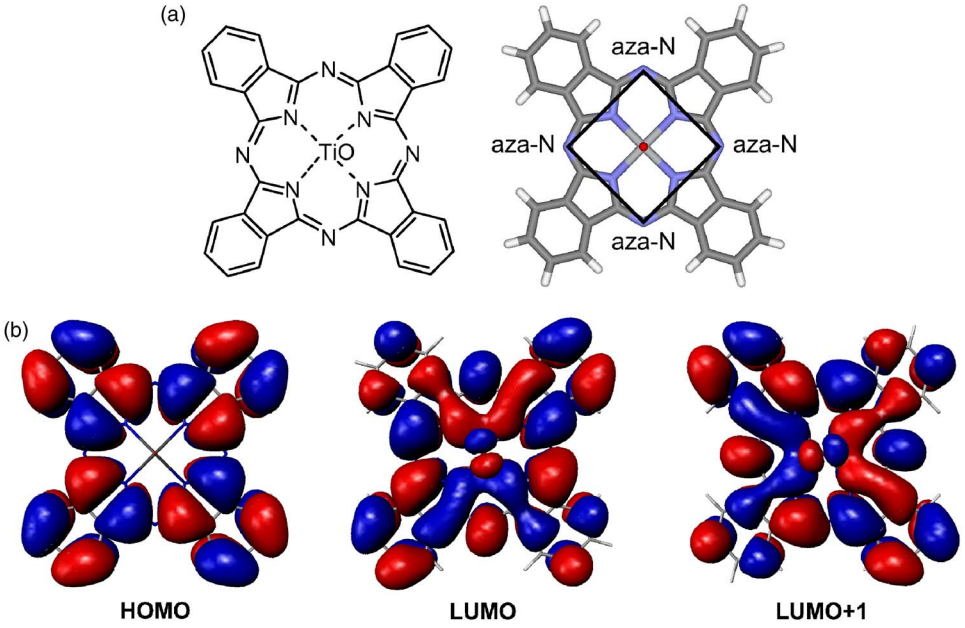


FIG. 1. (Color online) (a) TiOPc structural formula and molecular structure showing the plane formed by the aza-N atoms. (b) B3LYP/6-31G(*d*) HOMO and degenerate LUMO and LUMO+1 wave functions of the ground-state optimized geometry.

lar orbital (HOMO) levels of each molecule. For example, in the case of an infinite one-dimensional stack, the total bandwidth $W$ is equal to $4t$, where $t$ is the transfer integral. In a simple dimer model involving two interacting molecules, the splitting of the HOMO energy levels of each molecule is equal to $2t$. However, we stress that when the interacting molecules are not symmetrically equivalent, this approximation becomes inadequate due to site energy differences induced by effects such as polarization.[14] A more rigorous approach to obtaining the electronic coupling has thus been developed for the general asymmetric situation.[15] In this approach, the molecular orbitals of the dimer are described using a basis set of localized monomer orbitals. For systems where dimer HOMO and HOMO-1 levels are composed of only monomer HOMOs, the electronic coupling can then be calculated directly as the $H_{ij}$ matrix element obtained from the secular equation **HC**=**SCE**, where **H** is the system Hamiltonian (or Fock matrix), **C** is the eigenvector matrix, **S** is the overlap matrix of the monomer molecular orbital basis, and **E** is the diagonal eigenvalue matrix. We note that in more complicated cases involving contributions from other HOMO-$n$ or LUMO+$n$ levels, a more general definition of the transfer integral can be considered.[16]

In this study, we investigate the charge-transfer parameters for the triclinic phase II crystal of TiOPc ($\alpha$-TiOPc), with a focus on hole transport. The molecular structure of TiOPc is shown in Fig. 1 and the triclinic crystal structure, $\alpha$-TiOPc, is shown in Fig. 2. The unit cell of $\alpha$-TiOPc contains two inequivalent molecules that give rise to two types of interactions, namely, convex- and concave-type dimers. These are determined by the relative orientations of the protruding TiO groups, which force the usually planar structure of the phthalocyanine to adopt a nonplanar square pyramidal structure. The convex interactions involve TiOPc molecules with the protruding TiO groups and outwardly bowed $\pi$ systems facing each other, while the concave interactions involve inwardly bowed cofacial $\pi$ systems with the TiO groups oriented on opposite sides of the molecules, see Fig.

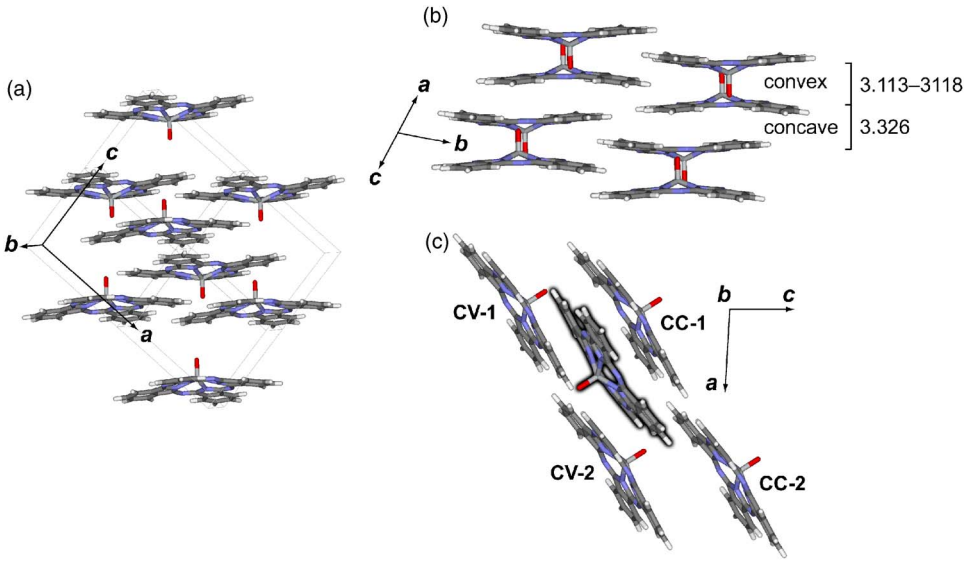


FIG. 2. (Color online) (a) The $\alpha$-TiOPc triclinic crystal system. (b) A view of the crystal structure showing interplanar separation distances, reported in angstroms (Å), between the concave- and convex-type dimers. (c) The four strongest interacting $\alpha$-TiOPc dimer pairs corresponding to two concave-type (**CC-1** and **CC-2**) and two convex-type (**CV-1** and **CV-2**) interactions viewed along the ***b*** direction of the crystal lattice.

2(b). Intermolecular distances between these dimers are short with interplanar separation distances measured from the planes formed by the four aza nitrogens (aza-N) occurring at 3.113–3.118 Å in convex dimers and 3.326 Å in concave dimers. Interacting $\pi$ systems in configurations where $\pi$-$\pi$ intermolecular distances are short can be expected to produce favorable charge-transport parameters for high charge mobilities. To the best of our knowledge, charge carrier mobility measurements on $\alpha$-TiOPc have not been reported.

## II. METHODOLOGY

Transfer integrals between specific dimers were calculated with DFT methods using the generalized gradient approximation and the PW91 functional with a DZP (DZ for Ti) basis set implemented in the ADF package[17] and at the B3LYP/6-31G($d$) level of theory in GAUSSIAN 03.[18] In both methods, molecular orbitals localized on each molecule are used as the basis set, and the orbital energies of the dimers are determined by the secular equation **HC=SCE** as described above. A basis set composed of monomer molecular orbitals can be used directly in ADF; however, GAUSSIAN 03 uses atomic orbital (AO) basis sets and requires a basis set transformation procedure in order to obtain the coefficient and overlap matrices of the molecular orbitals localized on each molecule.

The localized monomer orbitals can be projected onto the canonical molecular orbitals in the AO basis by a standard application of the projection operator,

$$|\psi_i\rangle\langle\psi_i|\psi_j\rangle = C_k|\psi_i\rangle, \tag{2}$$

where $|\psi_i\rangle = C_i|\varphi_i\rangle$ are the molecular orbitals of the isolated monomers in the AO basis $|\varphi_i\rangle$, and $|\psi_j\rangle = C_j|\varphi_j\rangle$ are the molecular orbitals of the dimer in the AO basis $|\varphi_j\rangle$. In matrix form, $\mathbf{C_i}$ is the block diagonal matrix containing the molecular orbital (MO) coefficients from each monomer with off block diagonals set to zero, and $\mathbf{C_j}$ is the matrix containing the MO coefficients of the dimer. A standard symmetric orthogonalization process can be applied to the basis set and Hamiltonian,[19] however, here the orbitals are orthogonalized following the calculation of the Fock matrix. Consequently, a block diagonal overlap matrix of the two monomers in the AO basis is contained in $\mathbf{S_i}$ with off block diagonals set to zero. The coefficient matrix $\mathbf{C_k}$ of the projected orbitals can then be obtained as

$$\mathbf{C_k} = \mathbf{C_i^T} \cdot \mathbf{S_i} \cdot \mathbf{C_j}, \tag{3}$$

where $\mathbf{C_i^T}$ indicates the transpose of $\mathbf{C_i}$.

The overlap between the localized molecular orbitals is calculated from the MO coefficients of the monomer orbitals and the overlap of the atomic orbitals in the dimer configuration. The overlap of the monomer orbitals is calculated in matrix form as

$$\mathbf{S_k} = \mathbf{C_i^T} \cdot \mathbf{S_j} \cdot \mathbf{C_i}, \tag{4}$$

where $\mathbf{S_j}$ is the overlap matrix of the atomic orbitals in the dimer configuration. Following basis set transformation, the Fock matrix can be solved using the MO coefficient and overlap matrices, $\mathbf{C_k}$ and $\mathbf{S_k}$, respectively. The electronic coupling element is represented as the matrix element $V_{ij} = \langle\psi_i|H|\psi_j\rangle$, which is then orthogonalized using Löwdin's symmetric transformation[20] as applied recently in the literature.[14]

Optimizations of monomer geometries and calculations of molecular reorganization energies were performed at the B3LYP/6-31G($d$) level of theory using GAUSSIAN 03 (Ref. 18) and a standard procedure detailed in the literature.[12]

The band structure of $\alpha$-TiOPc has been calculated using density functional theory in the generalized gradient approximation [GGA-PW91 (Ref. 21)] with a plane-wave basis set as implemented in the VASP program.[22] Electron-ion interactions were described using the projector augmented wave (PAW) method[23] with a kinetic-energy cutoff of 400 eV on the wave function expansion. Since hydrogen atoms were not included in the experimental crystal structure, hydrogen atoms were added and the ions in their instantaneous ground state were relaxed using a conjugate-gradient algorithm with the cell shape and volume fixed. Following optimization, the self-consistent calculations were computed with a $4\times4\times4$ $\boldsymbol{k}$ point mesh. The density of states (DOS) was computed using the tetrahedron method with Blöchl corrections. To corroborate the main features of the band structure described using GGA-PW91-PAW, the band structure was also computed for the relaxed geometry using the hybrid B3LYP functional with a 6-21G (6-31G for Ti) atomic orbital basis set implemented in the CRYSTAL06 program.[24]

It is known that DFT is unable to properly describe nonbonded interactions that contain substantial dispersion components.[25] These interactions are critical in determining binding energies as well as total energies, molecular geometries and orientations, and vibrational properties. Since electronic coupling is an overlap-dependent property, both B3LYP and PW91 are appropriate for evaluating transfer integrals and bandwidths in crystal structures. It has also been shown that constraining the lattice constants to experimental values during geometry optimizations effectively compensates for the errors in these interactions so that DFT calculations reproduce the molecular geometry and orientation,[26] and vibrational properties.[27]

## III. RESULTS

We have applied the generalized methodology above to calculate the effective transfer integrals for nearest neighbor molecular pairs in the $\alpha$-TiOPc crystal.[28] Band structure calculations were performed on the $\alpha$-TiOPc unit cell to explore the characteristics of a bandlike regime for charge transport.

### A. Transfer integrals and reorganization energy

Electronic coupling elements between all monomer HOMOs localized on nearest neighbor molecular pairs of $\alpha$-TiOPC were calculated with the PW91 functional. A total of 14 dimers were calculated and of these dimers, four molecular pairs gave electronic couplings larger than 0.010 eV and all others gave values that were less than 0.003 eV. The four strongly interacting dimer pairs are shown in Fig. 2(c) and correspond to two concave-type (**CC-1** and **CC-2**) and two convex-type (**CV-1** and **CV-2**) dimers. Alternating **CC-1**

TABLE I. Effective transfer integrals ($t_{eff}$) calculated for $\alpha$-TiOPc dimers with the PW91 and B3LYP density functionals.

| | $t_{eff,HOMO}$ (eV) | | $t_{eff,LUMO}$ (eV) | |
|---|---|---|---|---|
| Dimer | PW91/DZP/DZ[a] | B3LYP/6-31G(*d*) | PW91/DZP/DZ[a] | B3LYP/6-31G(*d*) |
| **CC-1** | −0.049 | −0.056 | −0.037 | −0.049 |
| **CC-2** | 0.011 | 0.011 | 0.008 | 0.009 |
| **CV-1** | −0.042 | −0.051 | −0.057 | −0.069 |
| **CV-2** | −0.136 | −0.164 | −0.033 | −0.044 |

[a]PW91 exchange potential with a DZP basis set (DZ for Ti).

and **CV-2** dimers occur along the ***a*** direction of the $\alpha$-TiOPc crystal, and alternating **CC-2** and **CV-1** dimers occur along the ***c*** direction. The effective transfer integrals calculated with the PW91 and B3LYP functionals are listed in Table I. The molecules in concave dimer **CC-2** are significantly more displaced than in **CC-1**; **CC-2** gives a correspondingly lower transfer integral (0.011 eV) in comparison with **CC-1** (−0.049 eV). The relative orientations of the **CV-1** and **CV-2** dimers are very similar and would be expected to give correspondingly similar electronic couplings; however, the couplings are notably different at −0.042 and −0.136 eV, respectively. For comparison, the electronic coupling between edge-to-face dimers in pentacene has been calculated to be a little more than twice as large [0.326 eV (Ref. 14)] as the electronic coupling for **CV-2**.

Perpendicular and lateral displacements in cofacial or near-cofacial arrangements have been investigated extensively and are known to be critical factors in determining electronic coupling.[12,29] A view perpendicular to the planes of the TiOPc molecules of the **CV-1** and **CV-2** dimers is shown in Fig. 3(a) and reveals slight differences in the lateral displacements of the molecules. The **CV-1** dimer is displaced along the *y* axis of the figure by 0.925 Å, and the **CV-2** dimer is displaced along the *y* axis by 0.068 Å. In the *x* direction, the **CV-1** and **CV-2** dimers are displaced by 7.418 and 6.849 Å, respectively.

To investigate the source of the difference in the **CV-1** and **CV-2** couplings, a model dimer configuration with a convex orientation was used to explore the effects of lateral displacements at a fixed perpendicular interplanar separation distance (3.1 Å) equal to that of the separation distances found in the crystal. The evolution of the transfer integral along these coordinates is shown in Fig. 3(b) and 3(c). Varying the *x* coordinate from 6 to 11 Å causes the electronic coupling to decrease from ~0.25 to 0 eV before quickly undergoing two changes in sign. The small increase around 6 Å and the subsequent decrease and changes in sign indicate a subtle oscillation in the wave function overlap, and thus in the electronic coupling, as the cofacial $\pi$ systems slip across each other. With the *x* coordinate fixed at 7.418 Å (the displacement along *x* in **CV-1**), the TiOPc molecules are displaced along the *y* coordinate from 0 to 12 Å in Fig. 3(c). The electronic coupling along this coordinate undergoes an oscillation beginning with maximum overlap of the four $\pi$ systems of the fused benzene rings followed by a decrease and change in sign as the two benzene units become staggered. As the molecules are displaced further, a second oscillation occurs as the $\pi$ systems of the remaining benzene rings slide across each other.

The PW91 electronic coupling between the HOMO levels in the **CV-2** dimer is more than three times as large as that of **CV-1**. The evolution of the transfer integral in a model dimer system indicates that large changes in the coupling strength occur as the convex TiOPc molecules are displaced from each other. For example, a displacement of 0.6 Å from 6.8 to 7.4 Å (difference in the **CV-1** and **CV-2** dimers) along the *x* coordinate causes a change of 0.09 eV in the transfer integral, and a change of 1.0 Å from the origin of the *y* coordinate causes a change of 0.07 eV. In both cases, the **CV-2** dimer lies closer to the maximum electronic coupling than **CV-1**, confirming that small variations in lateral

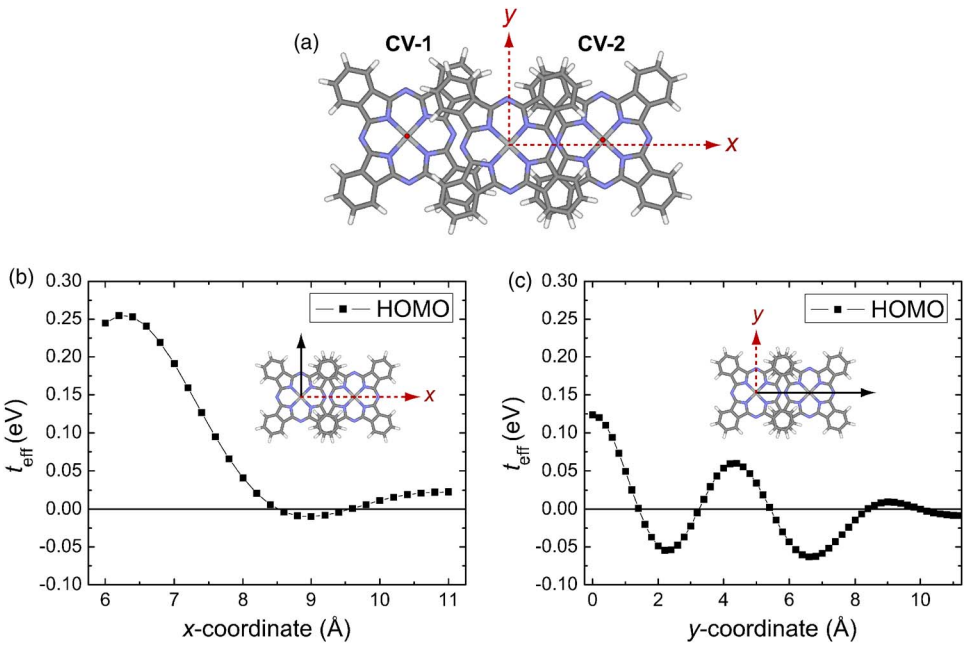


FIG. 3. (Color online) (a) View perpendicular to the TiOPc molecular planes in the **CV-1** and **CV-2** dimer configurations and evolution of the PW91 effective transfer integral $t_{eff}$ as a function of lateral displacement along the (b) *x* direction with *y* fixed at zero and (c) *y* direction with *x* fixed at 7.418 Å in a model dimer configuration with an interplanar separation distance of 3.1 Å.

displacements of the TiOPc molecules are responsible for the observed differences in electronic coupling. Applying a tight-binding approximation for an infinite one-dimensional stack of alternating **CC-1** and **CV-2** dimers, as occurs along the ***a*** direction, would lead to a hole bandwidth on the order of 0.37 eV with PW91/DZP/DZ and 0.44 eV with B3LYP/6-31G($d$). These values are on the same order as hole transport bandwidths calculated for rubrene ($\sim$0.340 eV),[30] for which hole mobilities of $\mu$(300 K $\sim$)20 $cm^2/V\,s$ have been reported.[31]

Electronic couplings between monomer lowest unoccupied molecular orbitals (LUMOs) were also calculated and are presented in Table I. We note that the electronic structure of the optimized TiOPc monomer consists of degenerate LUMO levels, shown in Fig. 1(b). However, in $\alpha$-TiOPc, significant molecular distortions occur in going from solution to the solid state that lift this degeneracy;[8] similar losses in degeneracy are found in the Y-form and phase I crystals of TiOPc. The lifting of LUMO degeneracy gives rise to splitting of the experimental absorption bands with the largest splittings in the $\alpha$-TiOPc and Y-forms.[8] We find that the LUMO of the monomer (in the geometry taken directly from the crystal structure) is significantly separated from its corresponding LUMO+1 (by 0.39 eV at the PW91/DZP/DZ level and 0.49 eV at the B3LYP/6-31G($d$) level). As a result, in the dimers, the LUMO and LUMO+1 levels are composed only of monomer LUMO levels. The transfer integrals between the LUMO levels of the monomers in the **CC-1**, **CC-2**, and **CV-1** dimers are comparable to their respective HOMO electronic couplings, while the **CV-2** LUMO dimer is four times smaller than the HOMO coupling. Applying a tight-binding approximation for an infinite one-dimensional stack of alternating **CC-1** and **CV-2** dimers would lead to an electron bandwidth on the order of 0.14 eV with PW91/DZP/DZ and 0.19 eV with B3LYP/6-31G($d$).

We also evaluated the internal reorganization energies associated with hole and electron transfer for TiOPc. B3LYP/6-31G($d$) values of 0.038 and 0.180 eV were obtained for hole and electron transfer, respectively. For comparison, reorganization energies for metal-free phthalocyanine (Pc) were calculated to be 0.044 and 0.188 eV for hole and electron transfer, respectively (essentially identical values of 0.045 and 0.186 eV have been reported using a slightly larger basis set at the B3LYP/6-31G($d$,$p$) level of theory).[32] Thus, the substitution by the TiO group is seen not to induce any significant changes in the internal reorganization energies relative to Pc. Remarkably, to our knowledge, the 0.038 eV hole transport reorganization energy calculated for TiOPc is the lowest reported to date; it is markedly lower than the values calculated for rubrene [0.159 eV at B3LYP/6-31G($d$,$p$) (Ref. 30)]. or for pentacene [0.098 eV at B3LYP/6-31G($d$) (Ref. 33) and 0.095 at B3LYP/6-31G($d$,$p$) (Ref. 34)].

### B. Band structure

The single crystal of $\alpha$-TiOPc is a triclinic system ($P$-1) with cell parameters of $a$=12.17 Å, $b$=12.58 Å, and $c$ =8.64 Å, and $\alpha$=96.3°, $\beta$=95.0°, and $\gamma$=67.9°, as shown in Fig. 2(a).[8] The electronic bands were calculated along the reciprocal lattice vectors and several specific paths on the boundary surfaces of the first Brillouin zone. The band structure and DOS spectrum calculated with the GGA-PW91-PAW method are presented in Fig. 4. All bands below the Fermi energy are filled and are separated from the conduction band by a direct band gap of 0.92 eV at the Γ point. Experimental band gaps determined by scanning tunneling spectroscopy and cyclic voltammetry (CV) methods have been reported at 2.04 and 2.03 eV under ambient conditions, respectively, and 1.72 eV with CV methods performed under inert conditions.[35] The band gap calculated from the B3LYP/6-31G($d$) ground-state optimized structure of the TiOPc monomer gives a value of 2.14 eV. The GGA-PW91-PAW method underestimates this value in comparison with experiment. While this is a usual drawback of GGA-DFT methods, the main features of the valence or conduction electronic structure are generally not affected.[36] In the remainder, we focus on the valence band.

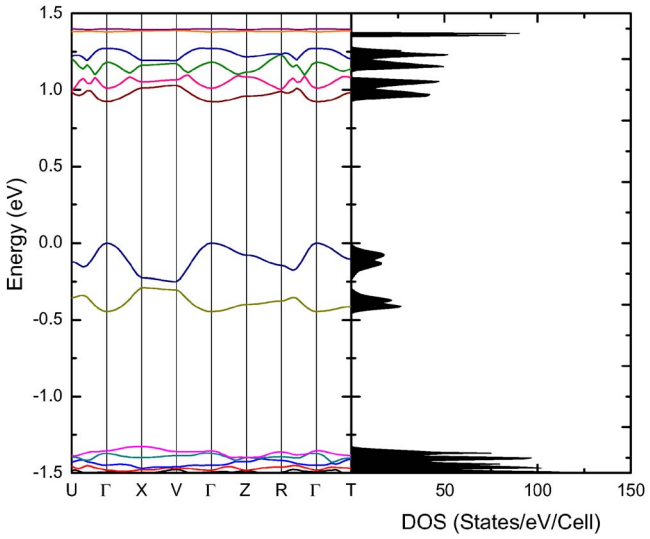


FIG. 4. (Color online) Band structure and DOS spectrum of $\alpha$-TiOPc calculated with the GGA-PW91-PAW method and a plane-wave basis set. The Fermi energy is taken as origin of the energy axis.

The valence band is composed of two subbands that arise from the presence of two inequivalent TiOPc molecules in the unit cell, and is well separated from other valence bands. The full bandwidth is 0.46 eV, which is consistent with but slightly larger than the 0.37 eV bandwidth derived from the tight-binding approximation for an infinite one-dimensional stack of alternating **CC-1** and **CV-2** dimers. Similar valence bandwidths have been obtained from band structure calculations on rubrene [$\sim$0.4 eV (Ref. 30)] and oligoacene single crystals.[37] The width and curvature of the upper valence band of $\alpha$-TiOPc remain larger and steeper than the lower portions of the conduction band, an indication that excess hole mobilities should be larger than excess electron mobilities.

The largest valence band dispersions occur along the Γ-X and V-Γ directions. The Γ-X direction corresponds to the $\mathbf{a}^*$ direction and includes alternating concave **CC-1** and convex **CV-2** dimers, seen clearly in Fig. 5(a). The V-Γ direction, shown in Fig. 5(b), corresponds to the $\mathbf{a}^*+\mathbf{b}^*$ direc-

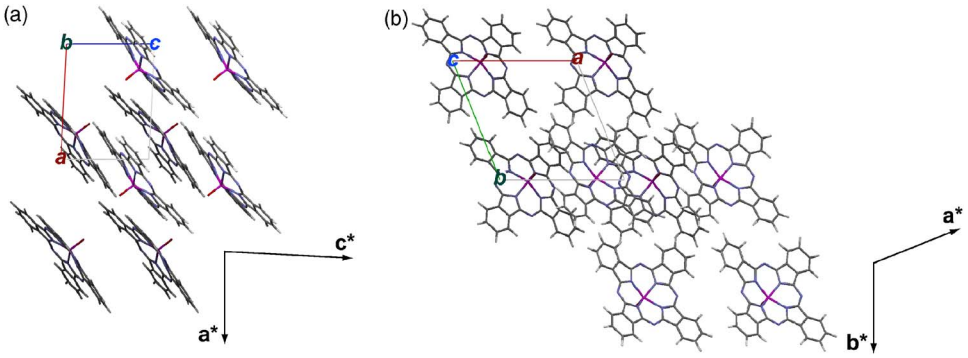


FIG. 5. (Color online) Crystal structure of $\alpha$-TiOPc viewed along the (a) ***b*** and (b) ***c*** directions of the crystal lattice with reciprocal lattice vectors shown at the bottom right.

tion and runs roughly parallel to the planes of the TiOPc molecules. Although this crystal direction is not easily correlated to specific dimer interactions, band dispersions approximately as large as those that occur along the Γ-X direction are generated. The Γ-Z direction corresponds to alternating **CC-1** and **CV-1** dimers along the $\mathbf{c}^*$ lattice vector. Relatively small amounts of band dispersion occur along this direction, which is consistent with the fact that $t_{\mathrm{eff,HOMO}}$ for these dimers is three times smaller than the **CV-2** dimer coupling.

The differences in band dispersion along the $\mathbf{a}^*$ and $\mathbf{c}^*$ crystal lattice vectors and variations in the coupling between dimers along these corresponding crystal directions indicate that hole mobility should exhibit anisotropy. Experimental measurements of hole mobilities for $\alpha$-TiOPc would be useful in determining mobility anisotropy and in confirming the calculated bandwidths obtained from band structure calculations.

## IV. SYNOPSIS

Electronic and band structure calculations have been used to characterize the charge-transport properties of the *p*-type semiconducting $\alpha$-TiOPc crystal. Our investigation of crystal structure dimers predicts that the largest electronic coupling occurs in convex-type dimers and that minor differences in lateral displacements yield significantly different coupling values. The strongest interactions occur between the HOMO levels of the monomers, and the reorganization energies for hole transport are lower than those calculated for pentacene and metal-free phthalocyanine.

Band structure calculations predict large hole transport bandwidths. Some of the largest dispersions occur along the high symmetry direction that correlates to alternating convex and concave dimers involving the **CV-2** dimer, for which the largest effective transfer integral was obtained. Calculated bandwidths are also found to correlate with a tight-binding approximation for a linear stack of alternating convex and concave dimers. A combination of electronic and band structure calculations has been used to investigate the favorable crystal packing phase of $\alpha$-TiOPc. The short intermolecular $\pi$-$\pi$ interactions are found to give rise to significant electronic couplings in dimer configurations and band dispersions in the crystal.

## ACKNOWLEDGMENTS

This work has been partly supported by the Office of Naval Research under Grant No. N00014-04-1-0120 and the CRIF Program of the National Science Foundation under Award No. CHE-0443564. We acknowledge stimulating discussions with Professor Neal Armstrong, Dr. Demétrio da Silva Filho, and Dr. Hong Li.

[1] K. Y. Law, Chem. Rev. (Washington, D.C.) **93**, 449 (1993).
[2] H. S. Nalwa, Adv. Mater. (Weinheim, Ger.) **5**, 341 (1993).
[3] Z. Bao, A. J. Lovinger, and J. Brown, J. Am. Chem. Soc. **120**, 207 (1998).
[4] R. H. Friend, R. W. Gymer, A. B. Holmes, J. H. Burroughes, R. N. Marks, C. Taliani, D. D. C. Bradley, D. A. Dos Santos, J. L. Brédas, M. Logdlund, and W. R. Salaneck, Nature (London) **397**, 121 (1999).
[5] C. W. Tang, Appl. Phys. Lett. **48**, 183 (1986); D. Wöhrle and D. Meissner, Adv. Mater. (Weinheim, Ger.) **3**, 129 (1991).
[6] H. Yonehara and C. Pac, Thin Solid Films **278**, 108 (1996).
[7] A. Yamashita, S. Matsumoto, S. Sakata, T. Hayashi, and H. Kanbara, J. Phys. Chem. B **102**, 5165 (1998).
[8] J. Mizuguchi, G. Rihs, and H. R. Karfunkel, J. Phys. Chem. **99**, 16217 (1995).
[9] H. Yonehara, H. Etori, M. K. Engel, M. Tsushima, N. Ikeda, T. Ohno, and C. Pac, Chem. Mater. **13**, 1015 (2001); H. Yonehara, K. Ogawa, H. Etori, and C. Pac, Langmuir **18**, 7557 (2002).
[10] M. Tsushima, Y. Motojima, N. Ikeda, H. Yonehara, H. Etori, C. Pac, and T. Ohno, J. Phys. Chem. A **106**, 2256 (2002).
[11] Z. D. Popovic, M. I. Khan, S. J. Atherton, A. M. Hor, and J. L. Goodman, J. Phys. Chem. B **102**, 657 (1998).
[12] J. L. Brédas, D. Beljonne, V. Coropceanu, and J. Cornil, Chem. Rev. (Washington, D.C.) **104**, 4971 (2004).
[13] R. A. Marcus, J. Chem. Phys. **24**, 979 (1956); R. A. Marcus, Rev. Mod. Phys. **65**, 599 (1993); R. A. Marcus and N. Sutin, Biochim. Biophys. Acta **811**, 265 (1985).
[14] E. F. Valeev, V. Coropceanu, D. A. da Silva Filho, S. Salman, and J. L. Brédas, J. Am. Chem. Soc. **128**, 9882 (2006).
[15] K. Senthilkumar, F. C. Grozema, F. M. Bickelhaupt, and L. D. A. Siebbeles, J. Chem. Phys. **119**, 9809 (2003).
[16] H. Li, J. L. Brédas, and C. Lennartz, J. Chem. Phys. **126**, 164704 (2007).
[17] G. Te Velde, F. M. Bickelhaupt, E. J. Baerends, C. Fonseca Guerra, S. J. A. Van Gisbergen, J. G. Snijders, and T. Ziegler, J. Comput. Chem. **22**, 931 (2001).
[18] M. J. Frisch, G. W. Trucks, H. B. Schlegel, G. E. Scuseria, M. A. Robb, J. R. Cheeseman, J. Montgomery, J. A. T. Vreven, K. N. Kudin, J. C. Burant, J. M. Millam, S. S. Iyengar, J. Tomasi, V. Barone, B. Mennucci, M. Cossi, G. Scalmani, N. Rega, G. A. Petersson, H. Nakatsuji, M. Hada, M. Ehara, K. Toyota, R. Fukuda, J. Hasegawa, M. Ishida, T. Nakajima, Y. Honda, O. Kitao, H. Nakai, M. Klene, X. Li, J. E. Knox, H. P. Hratchian, J. B. Cross, C. Adamo, J. Jaramillo, R. Gomperts, R. E. Stratmann, O. Yazyev, A. J. Austin, R. Cammi, C. Pomelli, J. W. Ochterski, P. Y. Ayala, K. Morokuma, G. A. Voth, P. Salvador, J. J. Dannenberg, V. G. Zakrzewski, S. Dapprich, A. D. Daniels, M. C. Strain, O. Farkas, D. K. Malick, A. D. Rabuck, K. Raghavachari, J. B. Foresman, J. V. Ortiz, Q. Cui, A. G. Baboul, S. Clifford, J. Cioslowski, B. B. Stefanov, G. Liu, A. Liashenko, P. Piskorz, I. Komaromi, R. L. Martin, D. J. Fox, T. Keith, M. A.

Al-Laham, C. Y. Peng, A. Nanayakkara, M. Challacombe, P. M. W. Gill, B. Johnson, W. Chen, M. W. Wong, C. Gonzalez, and J. A. Pople, GAUSSIAN 03, Revision B. 05, Gaussian, Inc., Wallingford CT, 2004.
[19] A. Szabo and N. S. Ostlund, *Modern Quantum Chemistry*, 1st ed. (McGraw-Hill, New York, 1989).
[20] P. O. Löwdin, J. Chem. Phys. **18**, 365 (1950).
[21] J. P. Perdew, J. A. Chevary, S. H. Vosko, K. A. Jackson, M. R. Pederson, D. J. Singh, and C. Fiolhais, Phys. Rev. B **46**, 6671 (1992); J. P. Perdew, J. A. Chevary, S. H. Vosko, K. A. Jackson, M. R. Pederson, D. J. Singh, and C. Fiolhais, Phys. Rev. B **48**, 4978 (1993).
[22] G. Kresse and J. Furthmueller, Phys. Rev. B **54**, 11169 (1996); G. Kresse and J. Furthmuller, Comput. Mater. Sci. **6**, 15 (1996); G. Kresse and J. Hafner, Phys. Rev. B **47**, 558 (1993); G. Kresse and J. Hafner, Phys. Rev. B **49**, 14251 (1994).
[23] P. E. Blöchl, Phys. Rev. B **50**, 17953 (1994); G. Kresse and D. Joubert, Phys. Rev. B **59**, 1758 (1999).
[24] R. Dovesi, V. R. Saunders, C. Roetti, R. Orlando, C. M. Zicovich-Wilson, F. Pascale, B. Civalleri, K. Doll, N. M. Harrison, I. J. Bush, P. D'Arco, and M. Llunell, CRYSTAL06, University of Torino, Torino, 2006.
[25] S. Tsuzuki and H. P. Luthi, J. Chem. Phys. **114**, 3949 (2001); Y. Zhao and D. G. Truhlar, J. Chem. Theory Comput. **1**, 415 (2005).
[26] K. Hummer, P. Puschnig, and C. Ambrosch-Draxl, Phys. Rev. B **67**, 184105/1 (2003).
[27] P. Hermet, J. L. Bantignies, A. Rahmani, J. L. Sauvajol, M. R. Johnson, and F. Serein, J. Phys. Chem. A **109**, 1684 (2005); G. J. Kearley, M. R. Johnson, and J. Tomkinson, J. Chem. Phys. **124**, 044514/1 (2006).
[28] W. Hiller, J. Straehle, W. Kobel, and M. Hanack, Z. Kristallogr. **159**, 173 (1982).
[29] J. L. Brédas, J. P. Calbert, D. A. da Silva Filho, and J. Cornil, Proc. Natl. Acad. Sci. U.S.A. **99**, 5804 (2002); J. Cornil, D. Beljonne, J. P. Calbert, and J. L. Brédas, Adv. Mater. (Weinheim, Ger.) **13**, 1053 (2001).
[30] D. A. da Silva Filho, E. G. Kim, and J. L. Brédas, Adv. Mater. (Weinheim, Ger.) **17**, 1072 (2005).
[31] V. Podzorov, E. Menard, A. Borissov, V. Kiryukhin, J. A. Rogers, and M. E. Gershenson, Phys. Rev. Lett. **93**, 086602 (2004).
[32] J. Tant, Y. H. Geerts, M. Lehmann, V. De Cupere, G. Zucchi, B. W. Laursen, T. Bjornholm, V. Lemaur, V. Marcq, A. Burquel, E. Hennebicq, F. Gardebien, P. Viville, D. Beljonne, R. Lazzaroni, and J. Cornil, J. Phys. Chem. B **109**, 20315 (2005).
[33] N. E. Gruhn, D. A. da Silva Filho, T. G. Bill, M. Malagoli, V. Coropceanu, A. Kahn, and J. L. Brédas, J. Am. Chem. Soc. **124**, 7918 (2002).
[34] M. Malagoli, V. Coropceanu, D. A. da Silva Filho, and J. L. Brédas, J. Chem. Phys. **120**, 7490 (2004).
[35] X. H. Kong, M. Wang, S. B. Lei, Y. L. Yang, and C. Wang, J. Mater. Chem. **16**, 4265 (2006).
[36] The band structure and DOS spectrum of $\alpha$-TiOPc were computed as well using the hybrid B3LYP functional with a 6-21 G (6-31 G for Ti) atomic orbital basis set implemented in the CRYSTAL06 program. The main features were fully consistent with those calculated using the GGA-DFT method in the VASP program (with a B3LYP direct band gap of 1.48 eV at the $\Gamma$ point and band dispersions that are slightly larger).
[37] Y. C. Cheng, R. J. Silbey, D. A. da Silva Filho, J. P. Calbert, J. Cornil, and J. L. Brédas, J. Chem. Phys. **118**, 3764 (2003).